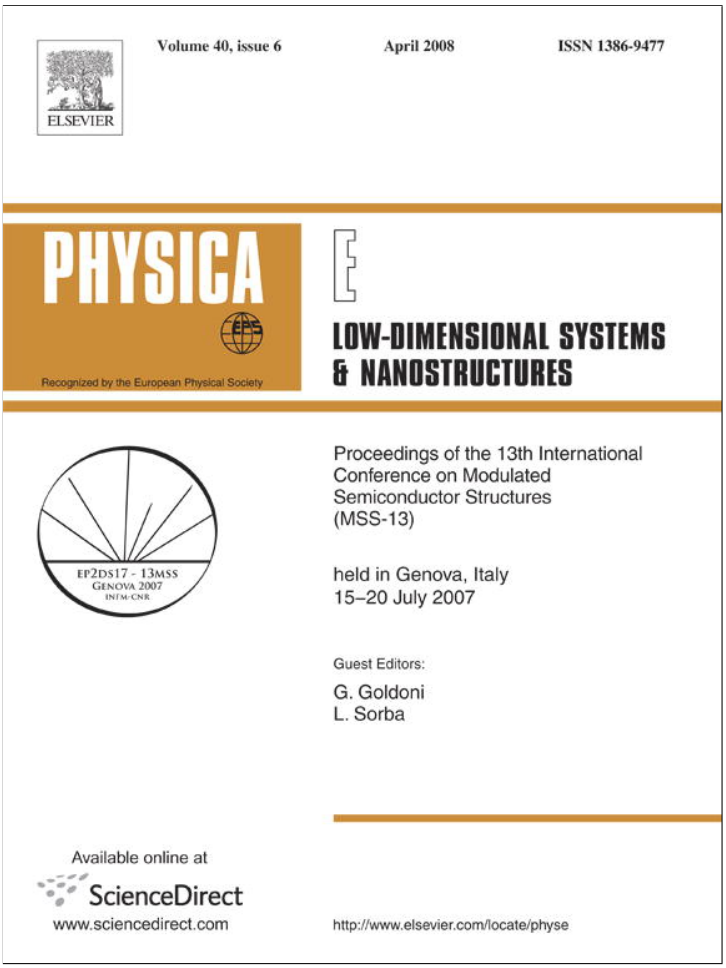

Available online at www.sciencedirect.com
ScienceDirect
Physica E 40 (2008) 1920–1923
PHYSICA E
www.elsevier.com/locate/physe

Localized strain effects on photoluminescence of quantum dots induced by nanoprobe indentation

Kazunari Ozasa[a,b,*], Mizuo Maeda[a], Masahiko Hara[a], Masane Ohashi[b], Yuan-Hua Liang[b], Hiroki Kakoi[b], Yoshio Arai[b]

[a]*RIKEN (The Institute of Physical and Chemical Research), 2-1 Hirosawa, Wako, Saitama 351-0198, Japan*
[b]*Saitama University, 255 Shimo-ookubo, Sakuraku, Saitama 338-8570, Japan*

Available online 21 September 2007

Abstract

We report localized strain effects on the low temperature (10 K) photoluminescence (PL) of self-assembled InGaAs/GaAs quantum dots (QDs), measured through an optical fiber nanoprobe (metal coated, aperture approximately 850 nm, flat apex). The localized strain is generated by the indentation of the nanoprobe onto the sample surface within elastic limit. The simultaneous measurement of the indentation force (typically <3 mN) and PL spectra enables us to perform the quantitative analysis of the strain effects through numerical model calculations. The energy-band shift calculated with 6×6 strain Hamiltonian for QDs and GaAs matrix figures out the accumulation of photoexcited holes at the edge region of the nanoprobe-indented area, which should be the mechanism of PL enhancement evoked by the nanoprobe indentation. The hole accumulation is caused by the shear strain components and thus not realized by the conventional hydrostatic experiments. The mechanism must be related closely to the emission enhancement reported for a p-type modulation doped laser.

PACS: 73.21.La; 78.55.−m; 78.55.Cr

Keywords: Nanoprobe; Strain; Quantum dots; Photoluminescence; Γ–X crossover; Indentation

1. Introduction

Strain induces various effects on semiconductor properties through the deformation of semiconductor-crystal lattices. Especially for nanostructures such as quantum dots (QDs), the localized strain often dominates their quantum energy levels, as in the case of strain-induced self-assembled QDs [1,2]. The typical techniques to measure the strain/pressure effects are the diamond anvil methods [3,4] and piezo-electric transducer methods [5]. These methods are established well, but cannot be applied for localized strains. Recently, we have reported nanoprobe-induced localized-strain effects on the photoluminescence (PL) of InGaAs/GaAs QDs embedded in a GaAs capping layer. A remarkable PL enhancement has been induced by the nanoprobe indentaion, which we attributed to the hole accumulation in the QDs due to the localized shear strain [6].

In this paper, we report the nanoprobe-induced strain effects on the PL of the QDs, focusing on the spatial distribution of PL enhancement and the quenching of PL. Numerical analysis is employed to figure out the strain-induced energy-gap shifts in InGaAs/GaAs system.

2. Experiments

Fig. 1 shows the schematic drawing of the nanoprobe indentation and PL measurements. In this study, we use probes with flat apex made with optical fibers with Au coatings. The apex is defined well by the focused ion beam (FIB) fabrication. The apex diameter is approximately 850/910 nm for Au-coated/uncoated nanoprobe (Fig. 1b and c).

*Corresponding author. RIKEN (The Institute of Physical and Chemical Research), 2-1 Hirosawa, Wako, Saitama 351-0198, Japan. Tel.: +81 48 462 1111x4444; fax: +81 48 462 4695.
E-mail address: ozasa@riken.jp (K. Ozasa).

1386-9477/$ - see front matter © 2007 Elsevier B.V. All rights reserved.
doi:10.1016/j.physe.2007.08.139

The indentation/scan of the nanoprobe is controlled through the driving voltage applied to conventional PZT probe-scanner in our STM-PL system [7]. The indentation force is measured by using a high-sensitivity load-cell (Tokyo Sokki, CLS-1NLS). The QDs are optically excited by a YAG laser (532 nm, 540 mW/cm^2), and PL spectrum is obtained by a monochromater (SPEX, 270M) and liquid-nitrogen-cooled charge coupled device (CCD; SPEX, CCD-2000). The measurement is performed at approximately 10 K with liquid helium cooling.

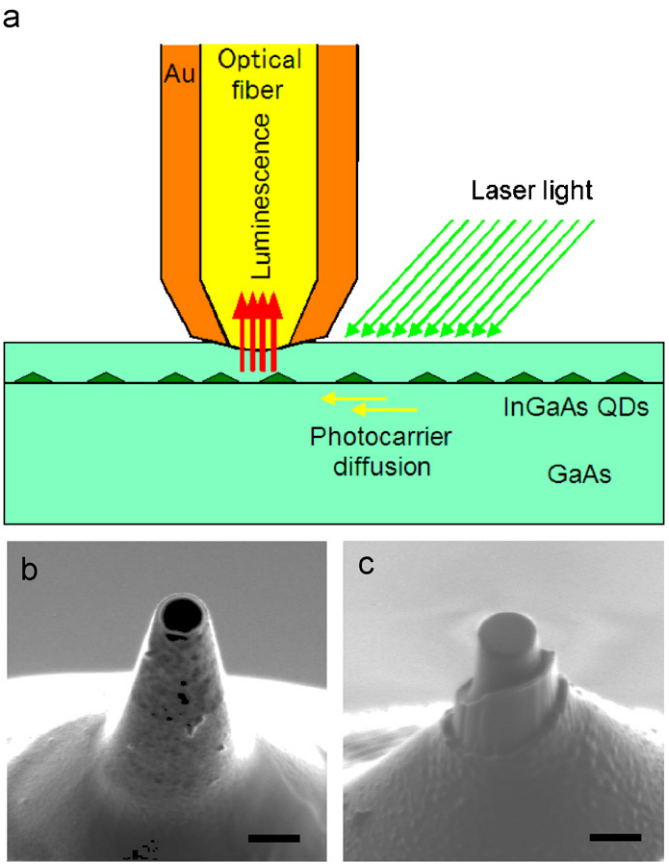

Fig. 1. (a) Schematic drawing of our nanoprobe PL/indentation measurement, (b) Au-coated probe, and (c) uncoated probe. (b, c) Scanning ion micrograph images with scale bar 1 μm.

The InGaAs/GaAs QDs measured in this report were fabricated by the strain-induced self-assembly technique with chemical beam epitaxy (480 °C) [8]. They have pyramid-like shapes [9] with approximately 20 nm in base width and 7 nm in height, and were embedded in GaAs capping layer of 50 nm in thickness. The density of QDs was 5–6 × 10^{10} cm^{-2} and chemical composition was $In_{0.5}Ga_{0.5}As$.

3. Results and discussion

The localized strain induced by nanoprobe indentation results in the energy-band-gap change of InGaAs/GaAs system. In order to figure out the distribution of shifts of energy band gap, the strain analysis and band-gap-shift calculation have been performed by employing finite element (FE) method. In the FE calculation, the elastic strain and the band-gap shift were calculated with a small deformation theory and 6 × 6 strain Hamiltonian of Pikus and Bir [10], respectively. The material parameters used were elastic constants of c_{11} (101.05/118.8 GPa for InGaAs/GaAs), c_{12} (49.53/53.8 GPa), and c_{44} (49.49/59.4 GPa), deformation potential of a_c (−6.06/−7.63 eV), a_v (−0.93/−1.00 eV), b (−1.81/−1.77 eV), d (−3.21/−3.10 eV) and Δ_0 (0.35/0.33 eV), respectively. Detailed description on FE model and calculation process can be found in our separate report [11].

Fig. 2 shows the 3D diagram for the band gap shift in GaAs obtained by the numerical analysis for the indentation force of 2.0 mN with 910-nm-diameter nanoprobe. The shift of conduction band minimum (CBM) is positive

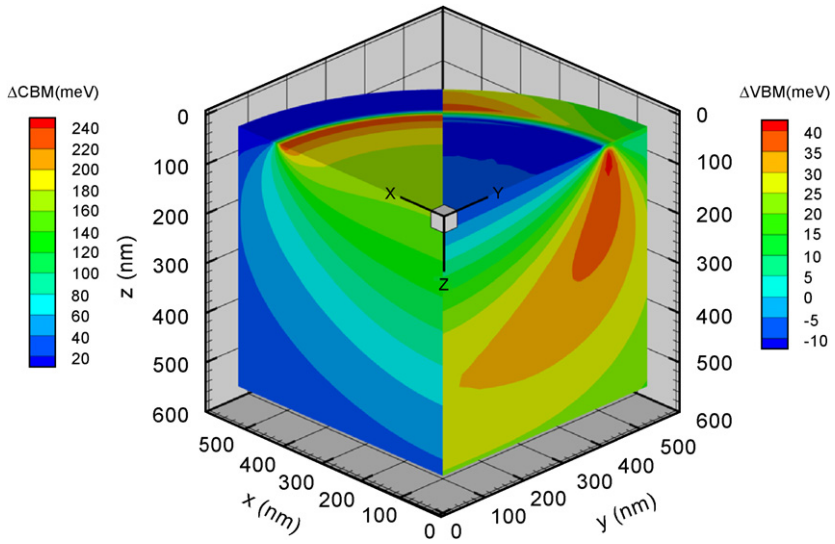

Fig. 2. Analysis of energy shift for CBM and VBM of GaAs matrix induced by the nanoprobe indentation of 1.3 mN. Probe center is at $(x, y) = (0, 0)$, the diameter is 850 nm, and the surface is at $z = 0$.

for all the area of the indentation, and highly positive at the surface of the edge region of the nanoprobe-indented area (contact-edge region, hereafter). On the contrary, the shift of valence band maximum (VBM) is negative at the shallow area beneath the indented nanoprobe, but positive at the other area. The positive VBM shift is concentrated especially at the shallow part of the contact-edge region, due to the localized shear strain for the flat apex nanoprobe. The distributions of CBM and VBM for the flat-apex nanoprobe are remarkably different from those for the rounded nanoprobe previously reported [6], where the topmost VBM lies beneath the center of the nanoprobe. The photoexcited holes are accumulated into the topmost part of the positively shifted VBM. Therefore, the enhanced PL of QDs is expected at the contact-edge region for the flat-apex nanoprobe.

In order to prove that the PL of QDs is enhanced in the contact-edge region, we performed the PL measurement with step-by-step change of the horizontal position of the nanoprobe (lateral scan). Fig. 3 shows the PL peak diagram obtained for the lateral scan of Au-coated nanoprobe with a constant indentation force of 1.3 mN. A total of 42 traces of PL peaks were analyzed by means of fitting of band-gap shift for the QDs (not for GaAs matrix) to identify the relative location of the QDs to the indented nanoprobe, as shown in Fig. 3 for the typical four of the 42 traces. The y_d shown in Fig. 3 means the distance from the scanning line of the center of the nanoprobe apex. The enhanced PL peaks are thus observed for the distance of $(y_d^2 + (\text{nanoprobe scan})^2)^{0.5}$ from the center of the nanoprobe apex. This analysis for 42 traces revealed that the PL enhancement is observed for the distance 360–450 nm from the center of the nanoprobe apex, i.e., in the contact-edge region (contact-edge line $-65 + 25$ nm). The results correspond well with the topmost part of positively shifted VBM in Fig. 2, and therefore we can conclude that the PL enhancement is caused by the accumulation of photoexcited holes due to the positive shifts of VBM by the nanoprobe indentation. The PL enhancement by the surface plasmon [12] is not the case for the nanoprobe-indentation PL-enhancement, because we also observed the PL enhancement with the nanoprobes without Au-coating (Fig. 1c). The hole accumulation induced by the nanoprobe indentation has similar effects as modulation p-type doping into the nanostructures (in this case, QDs). The modulation p-doping is considered to be effective to improve QD-laser performance [13], and therefore, the artificial modulation p-doping by the nanoprobe indentation is highly potential for the performance investigation on nanostructure-based devices.

Interestingly, the enhanced PL is quenched for the far larger indentation force. Fig. 4 shows the PL diagram versus indentation force, where the PL is enhanced above 0.2 mN and quenched above 3.1 mN. The quenched PL peaks appear again when the indentation force is reduced, as shown in unloading part in Fig. 4, revealing that the defect formation [14] is not the mechanism of the PL

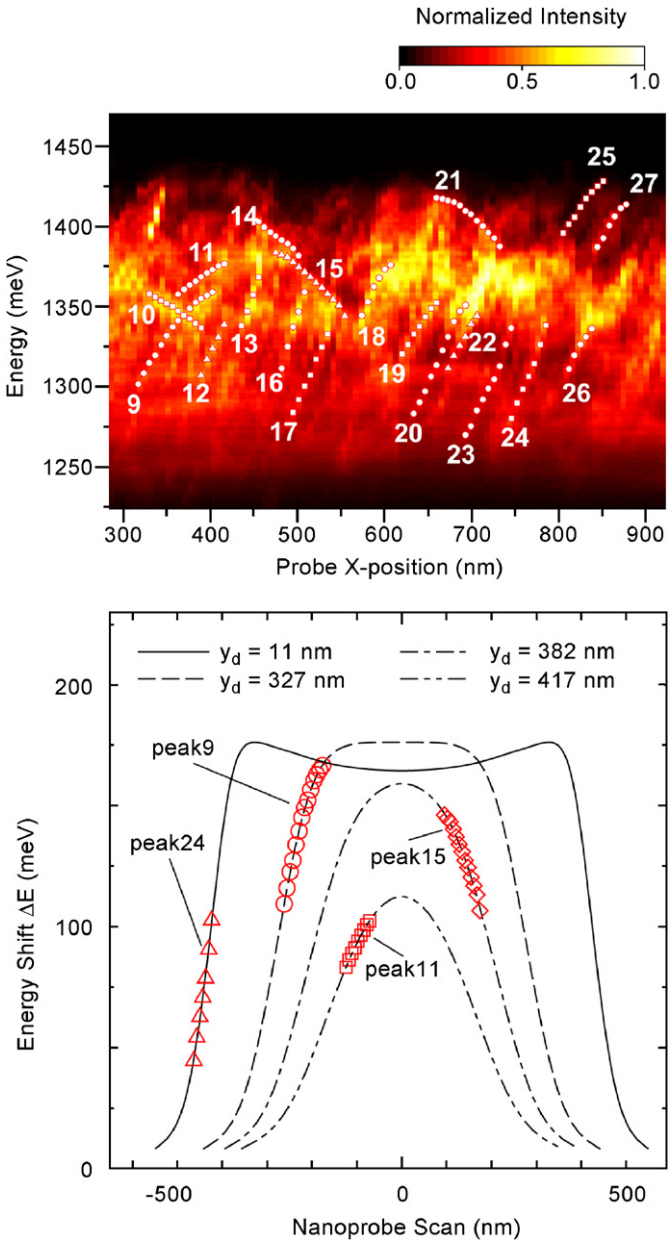

Fig. 3. PL diagram obtained by nanoprobe scan with indentation force of 1.3 mN with Au-coated nanoprobe (top). Fitting of energy shift as a function of distance from nanoprobe center (bottom). y_d represents the vertical distance from the scan line.

quench at higher indentation forces at least in our case. We previously attributed the PL quench to the de-tuning of the position of hole accumulation from the QDs location (depth) in the case of rounded nanoprobe [6]. However, the topmost part of positively shifted VBM is mostly independent of the indentation force in the case of the flat-apex nanoprobe. This excludes the de-tuning mechanism for the PL quench, and consequently suggests that the mechanism of PL quench at higher indentation forces should be Γ–X crossover [3], the reduction of confinement potential for electron/hole in the QDs, or the electron escape from the QDs due to the strong CBM bending.

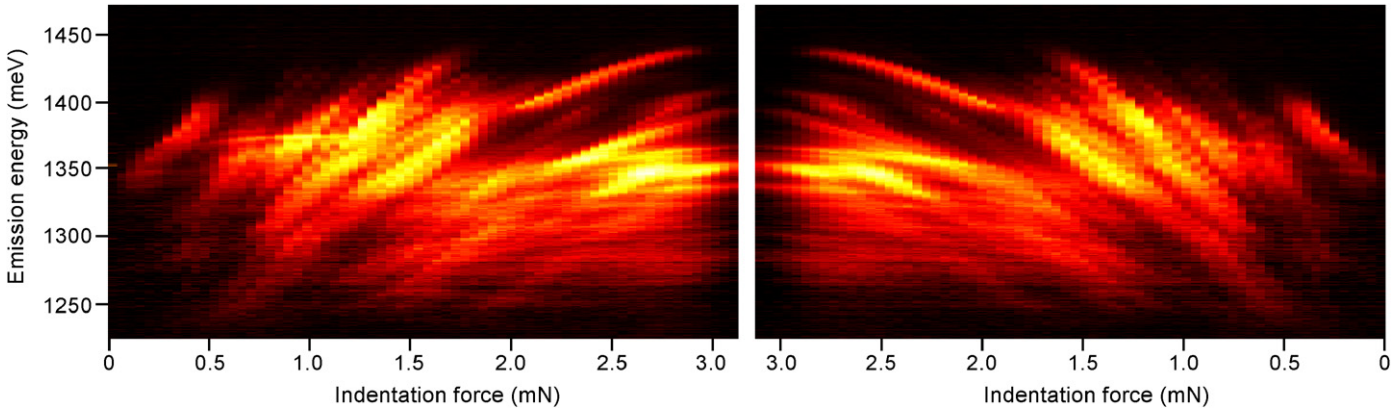

Fig. 4. PL diagram obtained by nanoprobe indentation (left) and following unloading (right), with uncoated nanoprobe.

The further investigation on the quench mechanism is now on going, and will be reported in the near future [15].

References

[1] J. Ahopelto, A. Yamaguchi, K. Nishi, A. Usui, H. Sakaki, Jpn. J. Appl. Phys., Part 2 32 (1993) L32.
[2] D. Leonard, M. Krishnamurthy, S. Fafard, J.L. Merz, P.M. Petroff, J. Vac. Sci. Technol. B 12 (1994) 1063.
[3] I.E. Itskevich, S.G. Lyapin, I.A. Troyan, P.C. Klipstein, L. Eaves, P.C. Main, M. Henini, Phys. Rev. B 58 (1998) R4250.
[4] C. Kristukat, A.R. Goñi, K. Pötschke, D. Bimberg, C. Thomsen, Phys. Status Solidi B 244 (2007) 53.
[5] S. Seidl, A. Hogele, M. Kroner, K. Karrai, A. Badolato, P.M. Petroff, R.J. Warburton, Physica E 32 (2006) 14.
[6] K. Ozasa, Y. Aoyagi, A. Yamane, Y. Arai, Appl. Phys. Lett. 83 (2003) 2247.
[7] K. Ozasa, Y. Aoyagi, Physica E 13 (2002) 212.
[8] K. Ozasa, Y. Aoyagi, Y.J. Park, L. Samuelson, Appl. Phys. Lett. 71 (1997) 797.
[9] K. Ozasa, Y. Aoyagi, M. Iwaki, H. Kurata, J. Appl. Phys. 94 (2003) 313.
[10] G.E. Pikus, G.L. Bir, Sov. Phys. Solid State 1 (1959) 1502.
[11] Y.H. Liang, M. Ohashi, Y. Arai, K. Ozasa, Phys. Rev. B 75 (2007) 195318.
[12] A.M. Mintairov, K. Sun, J.L. Merz, C. Li, A.S. Vlasov, D.A. Vinokurov, O.V. Kovalenkov, V. Tokranov, S. Oktyabrsky, Phys. Rev. B 69 (2004) 155306.
[13] O.B. Shchekin, D.G. Deppe, Appl. Phys. Lett. 80 (2002) 3277.
[14] H.T. Johnson, R. Bose, J. Mech. Phys. Sol. 51 (2003) 2085.
[15] K. Ozasa, Y.H. Liang, M. Ohashi, H. Kakoi, Y. Arai, unpublished.